

STUDY OF BOUNDARY LAYER FOR INCOMPRESSIBLE FLOW OVER AIRFOIL ON ULTRA LOW REYNOLDS NUMBER

Antônio Carlos Henriques Marques, achm@uffs.edu.br

José Laércio Doricio, doricio@usp.br

Departamento de Engenharia de Materiais, Aeronáutica e Automobilística

Escola de Engenharia de São Carlos - Universidade de São Paulo

Av. Trabalhador São-Carlense, 400 - Centro - CEP: 13560-970 - São Carlos - São Paulo - Brasil.

Abstract. *This work presents an application of the virtual boundary method for simulations with ultra-low Reynolds number over an profile NACA0012 airfoil type. The incompressible flow is solved through numerical solution of the Navier-Stokes equations (direct simulation - DNS), using a model of immersed boundaries to model the airfoil. This methodology allows the modeling of complex geometries immersed in the flow through two independent grids: one Eulerian to represent the fluid and a Lagrangian to model the fluid-structure interface. The analysis of the boundary layer is widely studied phenomena in turbulence, by definition, are observed in three-dimensional flows. This work treat of an approximation of laminar boundary layer in the case of two-dimensional flow. Results for modeling the laminar boundary layer are presented for the airfoil profile ,subject to attack angles 2, 8 and 30 degrees, and the phenomena of thickening of the boundary layer and the bubble separation are discussed..*

Keywords: *Virtual Boundary Method, DNS, laminar boundary layer, ultra-low Reynolds*

1. INTRODUCTION

The effects of the boundary layer and the phenomenon of turbulence are purely three-dimensional characteristics. As Ferziger (2000), the Direct Numerical Simulation (Direct Numerical Simulation - DNS) is the most accurate method to simulate turbulent flows. In a DNS, simply solve the Navier-Stokes equations and to treat exactly all the conditions imposed on the flow. To resolve all scales of turbulence is necessary a number of degrees of freedom, related to the number of points of the computational mesh, excessively high for Reynolds numbers of practical interest in aeronautical. Thus its application is restricted to flows until low Re numbers. However, the Micro Aerial Vehicle (MAV) design treat with ultra-low Reynolds number and DNS simulations become interesting. Still, the computational cost is high and, to a first approximation of the behavior of the boundary layer, because this it uses 2-D simulation. Although the transition and turbulent flow around a two-dimensional airfoil is inherently three- dimensional, the two-dimensional simulation still helps us gain a better understanding of the development of the flow separation, instability, and vortex shedding, Alam et al. (2010).

However not the most appropriate model to address the analysis of boundary layer and present significant errors for large attack angles, the approximate results serve to show the applicability of the method and provide parameters for the study of the flow with ultra-low Reynolds the number over profile NACA0012 airfoil, keeping in view the scarcity of data for this type of problem. The work of Mittal and Balachandar (1995) shows a comparison of results from simulations of 2-D and 3-D flow over a cylinder with elliptical base. As for drag, there is a variation of 1% to 39%, respectively attack angles of 0° and 45° , showing that, quantitatively, the drag coefficient in the 2-D simulation is greater than in 3-D simulation. Characteristics of the non-separated boundary, there are virtually no differences between the simulated 2-D and 3-D. The variation in drag coefficient occurs because of the Reynolds shear stress in 2-D simulation is significantly larger than in 3-D simulation. This is given by the Reynolds shear stress decrease with increasing three-dimensionality in the wake of circular cylinder ($260 < Re < 1500$).

This paper presents a computational study of steady state incompressible viscous fluid flow over a NACA 0012 airfoil with accurate and efficient code to perform simulations of complex geometry flow on a regular grid . Schematically, SILVESTRINI and LAMBALLAIS (2002), the main difficulty is to obtain an accurate description of the turbulent structure dynamics with a realistic shape of the body geometry. In engineering flow simulations, the description of the external geometry is traditionally favored by the use of body-fitted curvilinear or unstructured grids. The major drawbacks of such approach are the considerable increase of the computational cost and the significant degradation of the accuracy.

The strategy is to employ the methodology of immersed boundaries to model the airfoil, more specifically the method to study ribbled surfaces in turbulent flows, called Virtual Boundary Method (VBM). In recent years, many authors have implemented new cases and new variations of these techniques, Saiki and Biringen (1996), Silva et al. (2003), Marques et al. (2006), etc. In immersed boundary method, the domain is composed of an Eulerian mesh, used to represent the field of flow and a Lagrangian mesh, used to represent the immersed boundary. The interaction between the immersed boundary and the fluid is obtained via a smoothed Dirac delta function. The principle of the Virtual Boudary Method is in the application of a force field to the fluid so that it takes the same shape of the boundary immersed and speed of the flow. This is the classic model of the Virtual Boundary Method for non-slip boundary condition. The Virtual Boundary Method

Saiki and Biringen (1996), designates a class of boundary methods where the calculations are performed on a Cartesian mesh that does not fit the shape of the “virtual body” that serves as a barrier to the flow. The boundary conditions on the surface of the body are not enforced directly. Instead, an extra term, called the forcing term is added to the governing equations. The behavior of incompressible flows can be described by the Navier-Stokes equations, which undergo a process of coupling of the fields of pressure and speed in order to solve them properly. The fluid-structure interaction is modeled by Navier-Stokes equations and the Virtual Boundary Method via a Runge-Kutta for time integration and VONOS scheme for the discretization of spatial variables. One of the goals is to verify the efficiency of the numerical method by mapping the velocity profile in the vicinity of the airfoil for various attack angles. Through a preliminary study of boundary layer, the computational results are compared with results from literature and other simulator - Xfoil. The results for ultra-low Reynolds number analyse the behavior of separation bubble and the transition of laminar to turbulent flow.

2. FLOW CONFIGURATION AND PARAMETERS

The flight regime of micro-aircraft poses difficulties for the aerodynamic analysis and design, but little experimental or computation work exists for aerodynamic surfaces operating at ultra low Reynolds numbers. The reduced scale and low flight speeds of these vehicles result in Reynolds numbers on the order of 10^3 . Aerodynamics at these Reynolds numbers are considerably different from those of more conventional aircraft. The flow is laminar and viscously dominated. Boundary layers are quite thick, often reaching a significant fraction of the chord length. Flow separation is an issue, even at low angles of attack.

The analyses make use of three assumptions about the flow field. The flow is incompressible by the formulation of the flow solver, the flow is fully laminar, and the flow field is steady. The assumption of incompressibility is well justified for this application. The justification of the fully laminar flow assumption seems reasonable for the Reynolds number and geometry of interest (profile NACA0012 airfoil, Fig. 1). In the absence of separation, the flow will be entirely laminar. Even slight separation will likely result in laminar reattachment in a smooth airfoil.

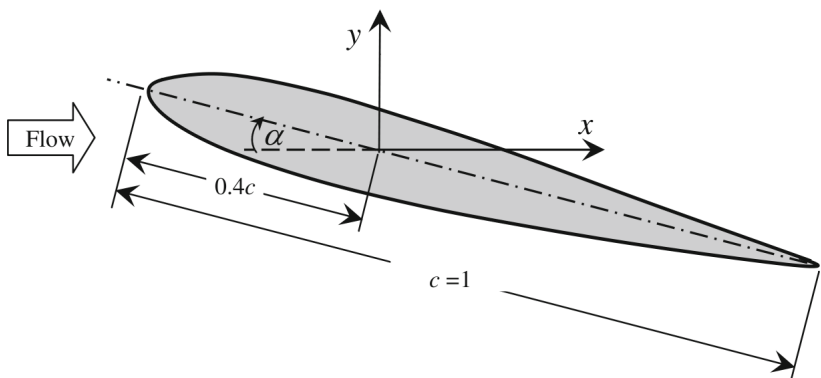


Figure 1. Illustration of profile NACA0012 airfoil (Alam et al, 2010)

We used a rectangular Cartesian mesh with non-regular grid 216×250 with $\Delta x_{min} = 0,01$, $\Delta y_{min} = 0,01$, $\Delta x_{max} = 0,35$ and $\Delta y_{max} = 0,35$ over a domain 6×3 dimensionless units, Marques et al. (2008). The geometric center of the NACA0012 airfoil was positioned at the coordinate point 1, 5 in direction x and 1, 5 in direction y , Fig. 2, with Reynolds number 1.000. The free-stream velocity u_{∞} , the free-stream pressure p_{∞} and the chord length of the airfoil c , are selected as the reference parameters for nondimensionalization. The upstream boundary is one chord lengths away from the leading edge of the airfoil. The upper and lower boundaries are about one chord lengths from the airfoil surface. The outflow boundary is located at four chord lengths downstream of the trailing edge. The no-slip condition is used on the surface of the airfoil.

The assumptions of the laminar boundary layer are: the thickness of the boundary layer is small enough rope to the profile ($c \gg \delta$); the component of the longitudinal velocity is greater than the transverse component ($u \gg v$); the transversal pressure gradient is neglected ($(\delta p \delta y) = 0$); the forces of weight are neglected; and the gradient of the longitudinal velocity in the transverse direction is much higher than the gradient speed transverse ($\delta u \delta y \gg (\delta v \delta y)$).

3. NUMERICAL METHODOLOGY

In this study an inviscid incompressible flow was considered in a two-dimensional rectangular domain Ω with an immersed boundary in the form of a simple closed curve Γ . The configuration of this curve will be represented in the

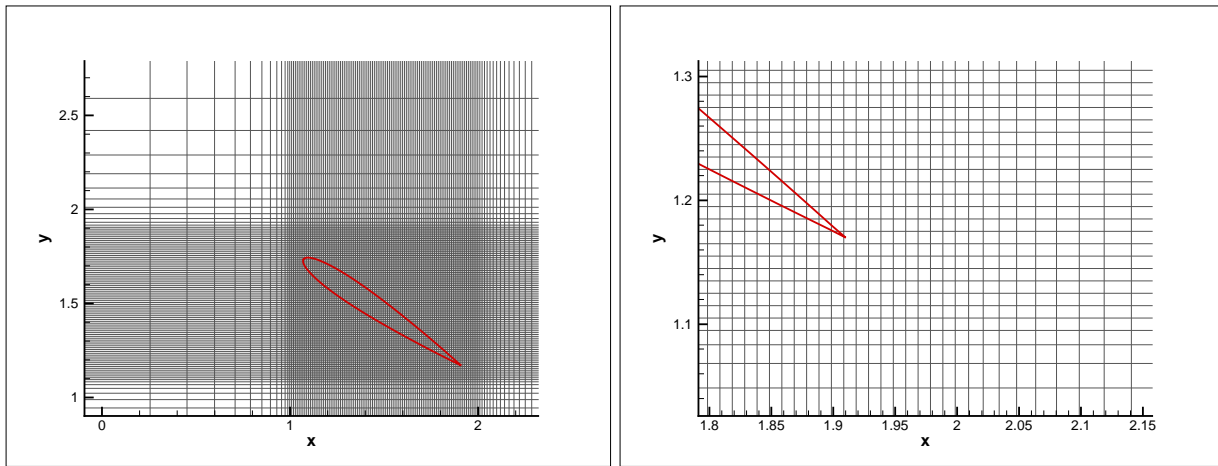


Figure 2. Illustration of mesh and NACA0012 airfoil

parametric form $\mathbf{X}(s, t)$, $0 \leq s \leq L_b$, $\mathbf{X}(0, t) = \mathbf{X}(L_b, t)$, where s is the surface point in the immersed boundary. Capital letters are used to represent the vector variables in the Lagrangian mesh. The governing equations in conservative form are given by:

$$\rho \left(\frac{\partial \mathbf{u}}{\partial t} + \mathbf{u} \cdot \nabla \mathbf{u} \right) + \nabla p = \mu \Delta \mathbf{u} + \mathbf{f}, \quad (1)$$

$$\nabla \cdot \mathbf{u} = 0, \quad (2)$$

$$\mathbf{f}(\mathbf{x}, t) = \int_0^{L_b} \mathbf{F}(s, t) \delta^2(\mathbf{x} - \mathbf{X}(s, t)) ds, \quad (3)$$

$$0 \approx \frac{\partial \mathbf{X}(s, t)}{\partial t} = \mathbf{u}(\mathbf{X}(s, t), t) = \int_{\Omega} \mathbf{u}(\mathbf{x}, t) \delta(\mathbf{x} - \mathbf{X}(s, t)) d\mathbf{x}, \quad (4)$$

$$\mathbf{u}(\mathbf{x}, t) \rightarrow \mathbf{u}_{\infty} \text{ com } |\mathbf{x}| \rightarrow \infty \quad (5)$$

In Eq.(1) to Eq.(5) $\mathbf{x} = (x, y)$ is the position vector, $\mathbf{u}(\mathbf{x}, t) = (u(\mathbf{x}, t), v(\mathbf{x}, t))$ is the velocity field of fluid and $p(\mathbf{x}, t)$ is the pressure field. The force actuating in the fluid (with respect to $d\mathbf{x} = dx dy$) is $\mathbf{f}(\mathbf{x}, t) = (f_1(\mathbf{x}, t), f_2(\mathbf{x}, t))$. Equations (1) and (2) are the two-dimensional incompressible Navier-Stokes equations. Equations (3) and (4) represent the interaction between fluid and the immersed boundary. The Delta Dirac function in both equations is a functional composed by two others delta functions, $\delta^2(\mathbf{x}) = \delta(x)\delta(y)$. In Eq.(3) the force is applied to the fluid by the immersed boundary.

3.1 Virtual Boundary Approach

The Virtual Boundary Method uses the finite differences in Eulerian-Lagrangian meshes for interaction between the fluid and the structure. Two distinct discretized meshes are necessary: a two-dimensional mesh to represent the fluid and a point mesh to represent the immersed boundary. The fluid variables are defined in an Eulerian mesh and a set of M Lagrangian points $\mathbf{X} = (X_k, Y_k)$ with $k = 0, 1, \dots, M - 1$ to discretize the immersed boundary, with initial grid spacing between the points $\Delta s = \frac{L_b}{M}$, where L_b is the curve Γ length. The force exerted in the boundary is defined on these points. It is important to observe that the points in the Eulerian mesh, which represent the fluid, are fixed while the points in the Lagrangian mesh, which represents the Virtual Boundary, are movable. The Virtual Boundary Method was used in an explicit scheme and the numerical solution is processed as follows:

1. The force field is calculated on the Lagrangian points with the initial conditions. The force $\mathbf{F}^n(s)$ is imposed in the Immersed Boundary and next the force $\mathbf{F}^n(s)$ is used in the force field of fluid to determine $\mathbf{f}^n(\mathbf{x})$ (Eq.(3)), using the following equation:

$$\mathbf{F}(\mathbf{X}(s), t) = \alpha \int_0^t (\mathbf{U}(\mathbf{X}(s), t) - \mathbf{V}(\mathbf{X}(s), t)) dt + \beta (\mathbf{U}(\mathbf{X}(s), t) - \mathbf{V}(\mathbf{X}(s), t)), \quad (6)$$

what guarantee that the fluid velocity is zero on the points, which define the no-slip boundary condition. The negative constants α and β will be chosen large enough in magnitude to bring the fluid velocity close to the interface velocity and are adjusted to obtain the expected physical behavior of the flow.

$$\mathbf{f}^n(\mathbf{x}) = \sum_s \mathbf{F}^n(s) \delta_h^2(\mathbf{x} - \mathbf{X}^n(s)) \Delta s, \quad (7)$$

where a discretized delta function is given by:

$$\delta_h^2(\mathbf{x}) = \delta_h(x)\delta_h(y), \quad (8)$$

with

$$\delta_h(r) = \begin{cases} \frac{1}{8h} \left(3 - \frac{2|r|}{h} + \sqrt{1 + \frac{4|r|}{h} - \frac{4r^2}{h^2}} \right), & |r| \leq h, \\ \frac{1}{8h} \left(5 - \frac{2|r|}{h} - \sqrt{-7 + \frac{12|r|}{h} - \frac{4r^2}{h^2}} \right), & h \leq |r| \leq 2h, \\ 0, & 2h \leq |r|. \end{cases} \quad (9)$$

This function was chosen because it presented better results in convergence order than others presented in the paper by Griffith and Peskin (2005).

2. The Navier-Stokes equations, defined by Eq.(1) and Eq.(2) with the force term $\mathbf{f}^n(\mathbf{x})$ to update the velocity field $\mathbf{u}^{n+1}(\mathbf{x})$, is solved by the fourth order Runge-Kutta method:

$$\begin{cases} \mathbf{V}_1^{n+\frac{1}{2}} = \mathbf{V}^n + \frac{1}{2}\Delta t \frac{\partial \mathbf{V}^n}{\partial t}, \\ \mathbf{V}_2^{n+\frac{1}{2}} = \mathbf{V}^n + \frac{1}{2}\Delta t \frac{\partial \mathbf{V}_1^{n+\frac{1}{2}}}{\partial t}, \\ \mathbf{V}_3^{n+1} = \mathbf{V}^n + \Delta t \frac{\partial \mathbf{V}_2^{n+\frac{1}{2}}}{\partial t}, \\ \mathbf{V}^{n+1} = \mathbf{V}^n + \frac{1}{6}\Delta t \left[\frac{\partial \mathbf{V}^n}{\partial t} + 2 \left(\frac{\partial \mathbf{V}_1^{n+\frac{1}{2}}}{\partial t} + \frac{\partial \mathbf{V}_2^{n+\frac{1}{2}}}{\partial t} \right) + \frac{\partial \mathbf{V}_3^{n+1}}{\partial t} \right], \end{cases} \quad (10)$$

where \mathbf{V} is a generic vector.

The spatial variables are solved using the projection method described in Harlow and Welch (1965). The convective derivatives are solved using the high order upwind method VONOS, described in Varonos and Bergeles (1998). The Navier-Stokes equations for viscous and incompressible flow in a Cartesian square domain Ω , containing an immersed boundary, can be modeled by equations (1), (2), (6) and (7). In this case \mathbf{F} is the external force imposed on the discrete surface points defined by $\mathbf{X}(s)$, \mathbf{U} is the fluid velocity at these surface points, and the velocity of the body itself is controlled by specifying $\mathbf{V} = (\mathbf{V}_{\mathbf{x}_b}, \mathbf{V}_{\mathbf{y}_b})$ at the boundary points (see Saiki and Biringen (1996)). In the present work the body does not move, i.e. $\mathbf{V} = \mathbf{0}$. The pressure and velocity coupling was solved using the projection method (see Harlow and Welch (1965)). The algorithm resolution is given by:

1. Calculate the force field $\mathbf{F}(\mathbf{X}(s), t)$, over the Lagrangian points $\mathbf{X}(s)$, using Eq.(6) and the initial conditions with constant β ;
2. Distribute the force $\mathbf{F}(\mathbf{X}(s), t)$ to the Eulerian grid using Eq.(7);
3. Calculate the fluid velocity field under the influence of the force field $\mathbf{f}(\mathbf{x}, t)$ using the projection method;
4. Verify if $\|\mathbf{E}\|_\infty \leq 10^{-6}$ where $\mathbf{E}_s = \|\mathbf{U}(s)\|_2$. If true go to step 5 else go to step 1.
5. Verify the continuity using Eq.(2).
6. Advance one time interval and go back to step 1.

4. RESULTS

The studies of external flows around bodies are of great importance, especially in cases of separation predicting. It occurs when the main stream separates from the surface of the body, and causes a large drag. A laminar boundary layer over a solid surface will separate as a result of curvature changes or adverse pressure gradient. With separated flows, the separation zone is complex and the characteristics of a separation structure may depend on whether the boundary layer is laminar or turbulent upstream of separation. To understand the basic characteristics of boundary layer separation, many investigators (as Lin and Pauley (1996)) have studied two-dimensional, steady, laminar separation. The separation phenomenon may be illustrated by Fig. (3)b.

The two-dimensional simulation starts from a uniform flow field, which is not the solution of the governing equations and may bring the initial perturbation resulting from the residual of the numerical solution. If this perturbation does not dissipate in the simulation, it may increase instability of the results of the two-dimensional simulation even though all the specified boundary conditions are steady and no external disturbances are enforced. Experimental values of NACA0012 airfoil behavior subject to incompressible flow for ultra-low Reynolds numbers are treated by HUANG et al. (2001) and

Purtell et al. (1981). In these works, there is variation in the attack angle up to 90° and an analysis of the separation bubble phenomenon. Considering the behavior of the velocity field, the figures (4) to (6) presents the contours of the mean streamwise velocity u for different α ($Re = 1000$). The region enclosed by $u = 0$ is characterized by negative u or a reversed flow. There seems to be an asymmetry in the reversal flow; the recirculating flow region near the leading edge appears larger than that near the trailing edge. The highest value obtained by HUANG et al. (2001), for Reynolds number $Re = 1200$, for $\frac{u}{u_\infty}$ was $\frac{u_{min}}{u_\infty} = 1.489$ to -0.34 . Purtell et al. (1981) obtained, for Reynolds number $Re = 1340$, $\frac{u_{min}}{u_\infty} = 0.382$. Computationally, for MFV and Reynolds number $Re = 1000$, we obtained $\frac{u_{min}}{u_\infty} = 0.5051$. The maximum velocities u_{max} in the leading and trailing-edge shear layers and the minimum velocity u_{min} in the recirculation are connected to drag; an increase in the magnitude of u_{max} and/or u_{min} corresponds to an increased drag, as table (1). Table (1) presents the dependence of C_L on a attack angle α and in Fig. (3)a the results are disposed with values presented for Alam et al. (2010) for $Re = 5.3 \times 10^3$.

Table 1. Computational results to drag coefficient and lift coefficient.

attack angle α	0	2	4	8	10	16	20	30
C_L	0	0.1221	0.2639	0.4254	0.4650	0.6644	1.0284	1.4444
C_D	0.1232	0.1239	0.1286	0.1590	0.2801	0.3006	0.5414	1.0537

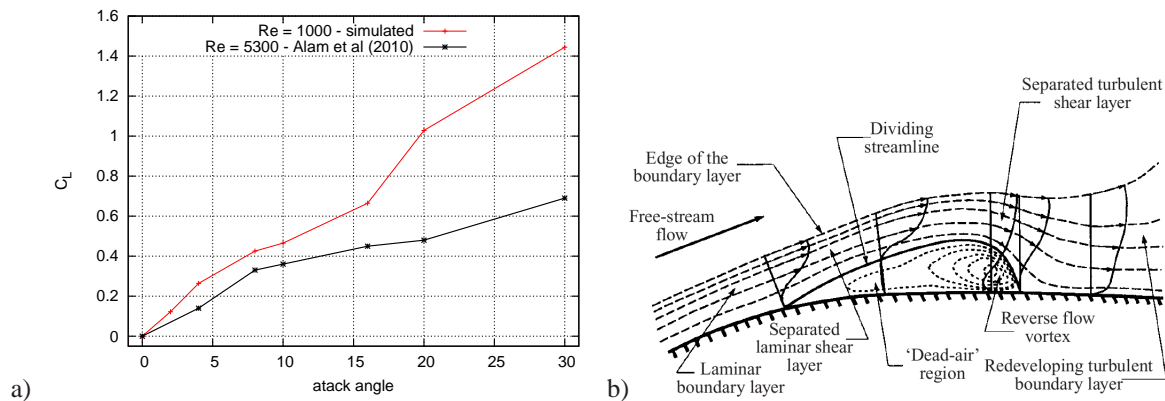


Figure 3. a) Dependence of C_L on α ; b) Scheme of laminar separation bubble (Horton 1968)

The evolution of the flow structure with increasing at ultra low Re has not been documented in the literature. HUANG et al. (2001) observed five different flows, depending on α ($0^\circ < \alpha < 90^\circ$) for $Re = 1.2 \times 10^3$ to 2.3×10^3 . The flow at $\alpha < 3^\circ$ corresponded to an attached flow, where the flow was completely attached on the entire length of the airfoil without the formation of vortices, as figure Fig. (4)a. The trailing edge vortex was observed at $3^\circ < \alpha < 8^\circ$, where the flow on the suction surface separated from the trailing edge, forming vortices, as figures Fig. (4)b and Fig. (5)a. At $8^\circ < \alpha < 17^\circ$, the boundary layer on the suction surface separated between the leading and trailing edges, forming vortices rolling on the surface, and eventually an alternate vortex street was established in the wake, as Fig. (5)b. At $17^\circ < \alpha < 60^\circ$, the boundary layer separating from the leading edge formed vortices, which grew in size as advected downstream, as Fig. (6)a. The contour of the instantaneous spanwise vorticity from the two-dimensional simulation, for $\alpha = 34^\circ$ is shown in Fig. (6)b, where the presence of the vortex shedding is visible on the upper surface of the airfoil. The laminar boundary layer starts near the leading edge of the airfoil and forms a separated shear layer, which becomes unstable due of large scale vortical structures. The vortices are generated through streamwise growth of the disturbance in the separated shear layer and the vortices are carried downstream by the mean flow along the airfoil surface. The present simulation do not show evidence of small scale vortical structures or flow transition. It is also interesting to note that the flow in the near wake contains shear layer as a result of the two flows with opposite vorticity sweeping off the upper and lower surface of the airfoil and the streamwise growth due the separated layer disturbance results and the shedding of vortices.

To check this phenomenon were analised 3 cases: attack angles $\alpha = 2^\circ$, $\alpha = 8^\circ$ e $\alpha = 34^\circ$, ie, the case where there is not separation - only laminar boundary layer; the case with the inicial instability formation, but no separation occurs, and the case where the separation occurs. Figures 7, 8 e 9 show the thickness boundary layer (δ^*), produced by VBM and software Xfoil, and u velocity component. The Xfoil model for calculating the boundary layer uses the integral method with Runge-Kutta scheme of 2^a order. Usually this procedure works well for $5 \cdot 10^5 < Re < 2 \cdot 10^7$, but was adapted by Drela (1988) for low Reynolds numbers with the following empirical criterion of transition:

$$Re_{\delta_2} > Re_{\delta_{2,crit}}, \quad (11)$$

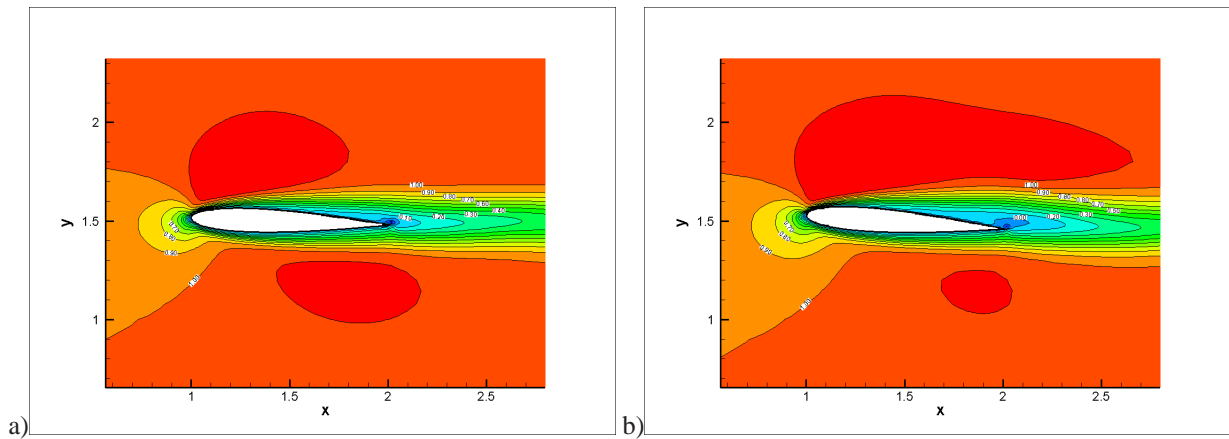


Figure 4. u velocity field: a) $\alpha = 2^\circ$; b) $\alpha = 4^\circ$.

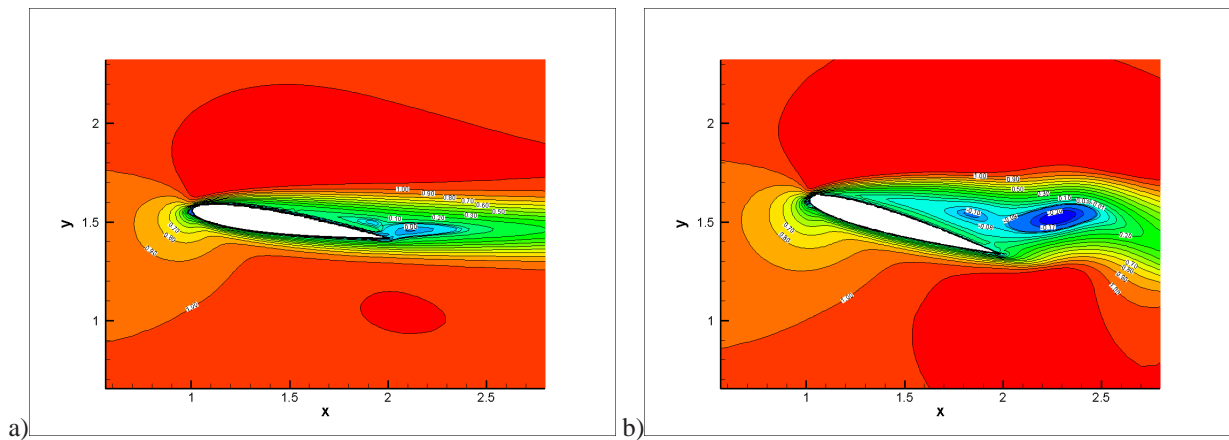


Figure 5. u velocity field: a) $\alpha = 8^\circ$; b) $\alpha = 16^\circ$.

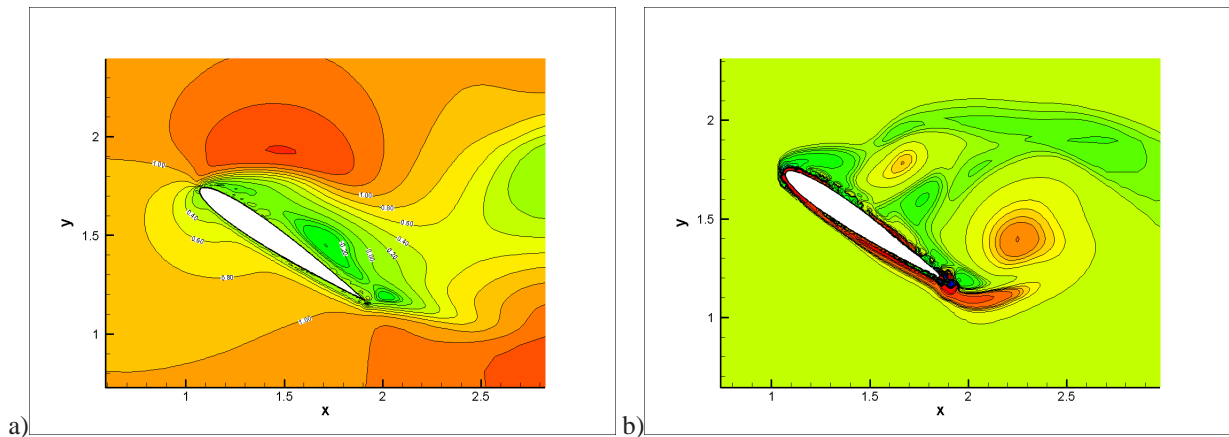


Figure 6. $\alpha = 34^\circ$: a) u velocity field for $\alpha = 34^\circ$; b) vorticity .

$$\frac{\delta \tilde{n}}{\delta Re_{\delta_2}} = 0.028 \cdot (H_{12} - 1) - \frac{0.0345}{e^{-\left(\frac{3.87}{H_{12}-1} - 2.52\right)^2}}, \quad (12)$$

$$\log_{10}(Re_{\delta_{2,crit}}) = 0.7 \cdot \tanh\left(\frac{14}{H_{12} - 1} - 9.24\right) + 2.492\left(\frac{1}{H_{12} - 1}\right)^{0.43} + 0.62 \quad (13)$$

where Re_δ is the Reynolds number for the thickness of momentum, \tilde{n} is the exponent of maxin Tollmien-Schlichting wave amplitude, H_{12} is the form factor $\frac{\delta_1}{\delta_2}$ with δ_1 displacement thickness of boundary layer, δ_2 thickness of momentum boundary layer. For the laminar case, the separation is assumed when $H_{23} < 1.51509$, where H_{23} form factor $\frac{\delta_3}{\delta_2}$ with δ_3 thickness loss energy.

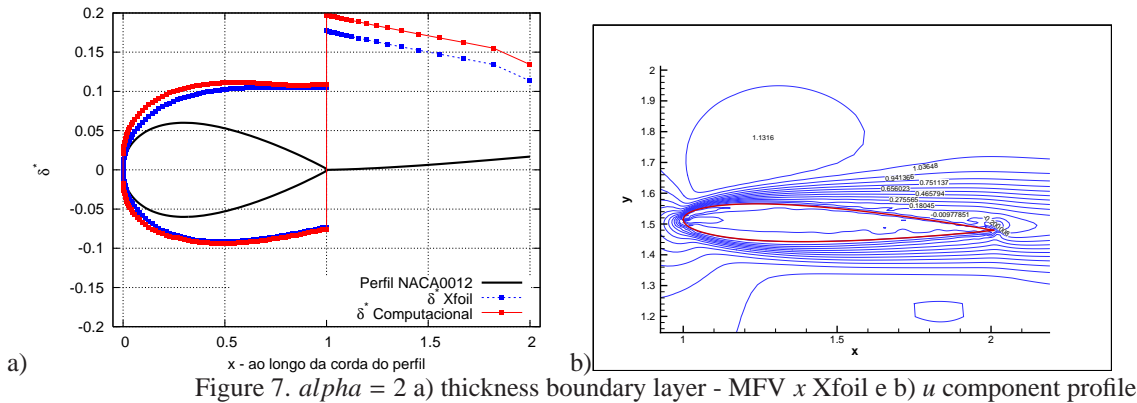


Figure 7. $\alpha = 2$ a) thickness boundary layer - MFV x Xfoil e b) u component profile

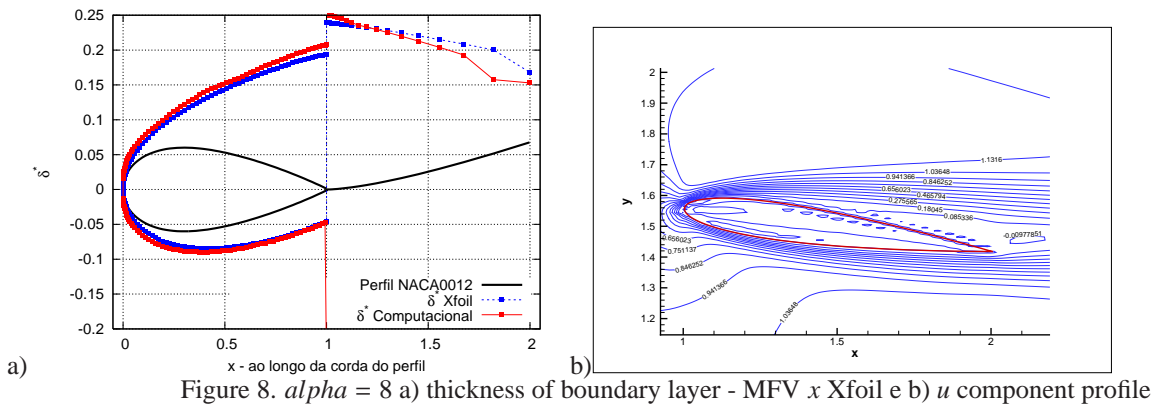


Figure 8. $\alpha = 8$ a) thickness of boundary layer - MFV x Xfoil e b) u component profile

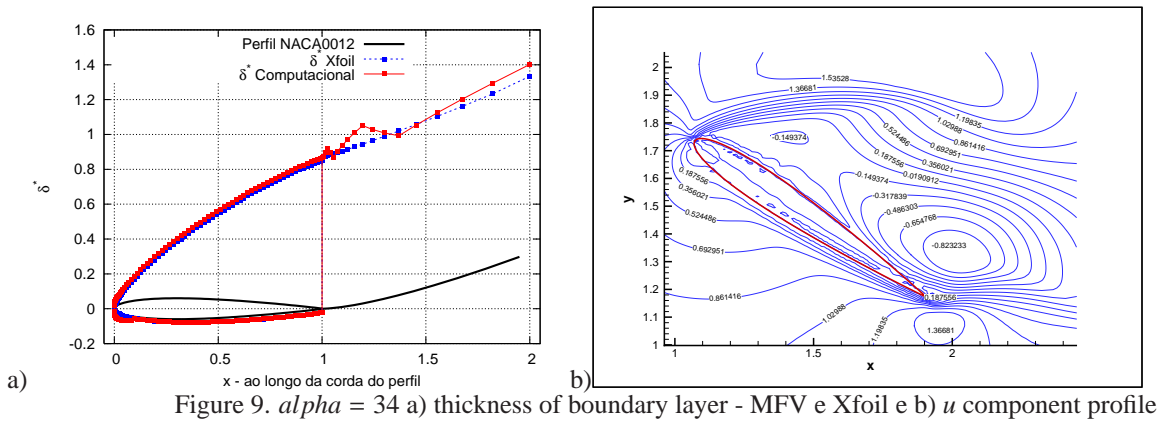


Figure 9. $\alpha = 34$ a) thickness of boundary layer - MFV e Xfoil e b) u component profile

As expected, for the attack angle $\alpha = 2$ there is no separation, only a small instability in the trailing edge due to the discontinuity of the airfoil geometry. For the attack angle $\alpha = 8$ occur the initial formation of separation, but there the changing of the boundary layer - just thickening the thickness. In the case of the attack angle $\alpha = 34$ occur the formation of the separation and vortices downstream of the trailing edge of the airfoil. In neither case was possible to observe the formation of the bubble separation, possibly because this phenomenon requires further mesh refinement.

5. CONCLUSIONS

Two-dimensional direct numerical simulation (DNS) has been carried out to study flow separation around a NACA 0012 airfoil with an attack angle of 2° , 4° , 8° , 16° , 34° and a Reynolds number of 10^3 . The incompressible Navier-Stokes equations which force field are solved by Virtual Boundary Method together with the central difference scheme, VONOS scheme and Neumann boundary conditions. The first sign of the instability appears in the near wake region and the disturbances in the near wake may propagate upstream and introduce a disturbance to the separated shear layer over the upper surface of the airfoil. The comparison between the numerical results shows that numerically computed ones agree with others authors to obtain the behavior of vortices wake and boundary layer. But, two-dimensional simulation do not appear to represent adequately the characteristics of the short separation bubbles. The Virtual Boundary Method presents itself as an efficient simulation for analysis of laminar boundary layer flow over NACA0012 airfoil with ultra low Reynolds number.

6. REFERENCES

- Alam, M. M., Zhou, Y., Yang, H. X., Guo, H., and Mi, J. 2010. The ultra-low Reynolds number airfoil wake. *Exp Fluids*, 48:81–103.
- Drela, M. 1988. Low-reynolds-number airfoil design for the m.i.t. daedalus prototype: A case study. *Journal of Aircraft*, 25(8):724–732.
- Ferziger, J. H. 2000. Simulation of Turbulence: Techniques and Possibilities. In *Anais da II Escola Brasileira de Primavera de Transição e Turbulência, ETT 2000*.
- Griffith, B. E. and Peskin, C. S. 2005. On the Order of Accuracy of the Immersed Boundary Method: Higher Order Convergence Rates for Sufficiently Smooth Problems. *Journal of Computational Physics*, 208:75–105.
- Harlow, F. and Welch, J. E. 1965. Numerical Calculation of Time-dependent Viscous Incompressible Flow of Fluid with a Free Surface. *Phys. Fluids*, 8:2182–2189.
- HUANG, R. F., WU, J. Y., JENG, J. H., and CHEN, R. C. 2001. Surface flow and vortex shedding of an impulsively started wing. *Journal of Fluid Mechanics*, 441:265–292.
- Lin, J. M. and Pauley, L. L. 1996. Low Reynolds number separation on an airfoil. *AIAA Journal*, 34:8–12.
- Marques, A. C. H., Doricio, J. L., Bueno, A. P. F., Greco Júnior, P. C., and de Souza, L. F. 2006. Numerical Simulation of two-dimensional Flows Over a Circular Cylinder: Immersed Boundary and Virtual Boundary Methods. In *Proceedings of the 27th Latin American Congress on Computational Methods in Engineering*.
- Marques, A. C. H., Doricio, J. L., and Greco Júnior, P. C. 2008. Método da Fronteira Virtual: simulação de escoamento incompressível sobre aerofólio NACA0012 com malha não uniforme. In *Proceedings of the 29th Iberian Latin American Congress on Computational Methods in Engineering*.
- Mittal, R. and Balachandar, S. 1995. Effect of three-dimensionality on the lift and drag of nominally two-dimensional cylinders. *Physics of Fluids*, 7(8):1841–1865.
- Purtell, L. P., Klebanoff, P. S., and Buckley, F. T. 1981. Turbulent boundary layer at low Reynolds number. *Phys. Fluids*, 24(5):802–811.
- Saiki, E. M. and Biringen, S. 1996. Numerical Simulation of a Cylinder in Uniform Flow: Application of a Virtual Boundary Method. *Journal of Computational Physics*, 123:450–465.
- Silva, A. L. F. L., Silveira-Neto, A., and Damasceno, J. J. R. 2003. Numerical Simulation of Two-Dimensional Flow over a Circular Cylinder Using the Immersed Boundary Method. *Journal of Computational Physics*, 189:351–370.
- SILVESTRINI, J. H. and LAMBALLAIS, E. 2002. Direct Numerical Simulation of Wakes with Virtual Cylinders. *International Journal of Computational Fluid Dynamics*, 16(4):305–314.
- Varonos, A. and Bergeles, G. 1998. Development and Assessment of a Variable Order Non-Oscillatory Scheme for Convection Term Discretization. *International Journal for Numerical Methods in Fluids*, 26:1–16.

7. Responsibility notice

The authors are the only responsible for the printed material included in this paper.